Observations of Multi-Resonance Effect in ELM Control with Magnetic Perturbation Fields on the JET Tokamak

Y. Liang*,[1] C. G. Gimblett,[2] P. K. Browning,[3] P. Devoy,[3] A. Alfier,[4] C. Giroud,[2] D. Harting,[1] H. R. Koslowski,[1] S. Jachmich,[5] Y. Sun,[1] C. Wiegmann,[1] T. Zhang,[1] and JET-EFDA contributors†
(JET-EFDA, Culham Science Centre, OX14 3DB, Abingdon,UK)

[1]*Forschungszentrum Jülich GmbH, Association EURATOM-FZ Jülich, Institut für Energieforschung - Plasmaphysik, Trilateral Euregio Cluster, D-52425 Jülich, Germany*
[2]*EURATOM/CCFE Fusion Association, Culham Science Centre, Abingdon, Oxon, OX14 3DB, UK*
[3]*School of Physics and Astronomy, University of Manchester, Manchester, UK*
[4]*Associazione EURATOM-ENEA sulla Fusione, Consorzio RFX Padova, Italy*
[5]*Association EURATOM-Belgian State, Koninklijke Militaire School - Ecole Royale Militaire, B-1000 Brussels Belgium*

Abstract: Multiple resonances of the ELM frequency caused by application of low n (= 1 or 2) magnetic perturbations for Edge Localized Mode (ELM) control has been observed on JET. With a low n field applied, a strong increase in ELM frequency, f_{ELM}, by a factor of ~ 4.5 was found in many separated narrow windows of q_{95} (resonant q_{95}), while the f_{ELM} increased only by a factor of ~ 2 for non-resonant q_{95} values. Both the global effect (no q_{95} dependence) and the multi-resonance effect (strong q_{95} dependence) depend on the amplitude of the perturbation field. The fractions of increase in f_{ELM} with different resonant q_{95} values are not the same. An analysis of ideal external peeling modes shows that both the dominant unstable peeling mode number and f_{ELM} depend on the amplitude of the normalized edge current density as well as the edge safety factor, q_a.

1. Introduction The periodic and transient power load onto the plasma facing components caused by type-I edge-localized modes (ELMs) in high performance H-mode plasmas [1] is a critical issue for the integrity and lifetime of these components in future high power H-mode devices, such as the International Tokamak Experimental Reactor (ITER) [2]. Accordingly, significant effort on both experimental investigations [3, 4] and the development of theoretical models [5, 6] has contributed towards understanding ELM physics and control.

In the past few years, active control/suppression of ELMs using resonant magnetic perturbation (RMP) fields has become an attractive method for application on ITER. DIII-D has shown that type-I ELMs are completely suppressed in a single narrow range of the edge safety factor ($q_{95} = 3.5 - 3.9$ or ~ 7.2) when even or odd parity $n = 3$ fields induced by a set of in-vessel coils are applied [7, 8]. A strong reduction in pedestal density by $\sim 40\%$ (the so called density pump-out effect) with $n = 3$ field was observed. An edge pedestal stability analysis shows that peeling-ballooning modes are stabilized due to a reduction in pedestal pressure gradient with $n = 3$ fields [7].

On JET, active control of the frequency and size of the type-I ELMs has been achieved

* Email: y.Liang@fz-juelich.de
† See the Appendix of F. Romanelli et al., paper OV/1-3, this conference

by applying a low n ($= 1, 2$) field induced by the Error Field Correction Coils (EFCC) system [9, 10]. When an $n = 1$ field is applied during the stationary phase of a type-I ELMy H-mode plasma, the ELM frequency, f_{ELM}, increases by a factor of $4 - 5$, while the ELM energy loss normalised to the total stored energy, $\Delta W_{ELM}/W$, decreases from 7% to values below the resolution limit of the measurement ($< 2\%$). Although similar impacts on the plasma, such as plasma density pump-out effect and magnetic rotation braking, are observed in RMP ELM suppression/control experiments on DIII-D and JET, no complete ELM suppression was observed to date with a low n field on JET, even with a Chirikov parameter [11] above 1 in the edge layer $\sqrt{\Psi} \geq 0.925$ [12]. This raises the question on the role of the perturbation spectrum in ELM control using RMP fields.

Recently, multiple resonances in the ELM frequency as a function of the edge safety factor q_{95} have been observed for the first time with an applied low n field on JET [13]. This experimental result suggests that there are two effects of the RMP on the ELM frequency: a **global effect** and the **multi-resonance effect**. The RMP global effect, which has no q_{95} dependence, results in a relatively weak increase of f_{ELM}. In contrast to the global effect, the RMP multi-resonance effect depends strongly on q_{95} and causes a stronger increase of f_{ELM}. These two effects are most likely due to different physics mechanisms. A model which assumes that the ELM width is determined by a localised relaxation triggered by an unstable ideal external peeling mode can qualitatively predict the observed resonances when low n fields are applied.

In this paper, further detailed comparisons of the low n fields effects on the plasma core and edge pedestal profiles between discharges with a resonant and a non-resonant q_{95} are presented in section 2.1. More recent experimental results of the multi-resonance effect observed in a wide q_{95} range from 3 to 5.5 with an increased amplitude of the $n = 2$ fields are described in section 2.2. For understanding the multi-resonance effect, the edge current density dependence of the stability of the ideal peeling modes is discussed in section 3.

2. Experimental observation On JET, the EFCC system, which was originally designed for compensation of the $n = 1$ intrinsic error field, has been used to create either $n = 1$ or $n = 2$ perturbation fields in ELM control experiments. Comparison of the effective radial RMP amplitudes, $|b_{res}^{r,eff}| = |B_{res}^{r,eff}/B_0|$, calculated for $n = 1$ and $n = 2$ configurations with the same EFCC coil current (I_{EFCC}) shows that the amplitude of $|b_{n=2}^{r,eff}|$ in the $n = 2$ configuration is a factor of ~ 3 smaller than $|b_{n=1}^{r,eff}|$ in the $n = 1$ configuration for all radii[12]. Here, $B_{res}^{r,eff}$ and B_0 are the radial resonant magnetic perturbation field (calculated with a vacuum approximation) and the on-axis toroidal magnetic field, respectively.

In the experiments presented in this paper, a target plasma with a low triangularity shape (lower $\delta \sim 0.2$) and a toroidal field (B_t) of 1.84 T was chosen. A stationary type-I ELM H-mode plasma with low electron collisionality at the edge pedestal ($\nu^* \sim 0.1$) was sustained by neutral beam injection (NBI) with a total power of 11.5 MW. In this experiment, no additional gas fuelling was applied during the H-mode phase. The q_{95} scan was carried out by varying the plasma current (I_p) only. The electron temperature and density profiles were measured by high resolution Thomson scatting (HRTS) and the core ion temperature and plasma toroidal rotation profiles were measured by charge exchange spectrometry (CXS).

2.1 Multi-resonance effect with $n = 1$ fields A comparison of two JET ELM control pulses using the same $n = 1$ field but different q_{95} of 4.5 ($I_p = 1.4$ MA) and 4.8 ($I_p = 1.32$ MA) is shown in figure 1. A similar f_{ELM} of ~ 20 Hz was observed in these two discharges before the $n = 1$ field was applied. The $n = 1$ field created by the EFCCs had a ramp-up phase of I_{EFCC} for 300 ms and a flat-top with $I_{EFCC} = 32$ kAt for 2.5 s, which

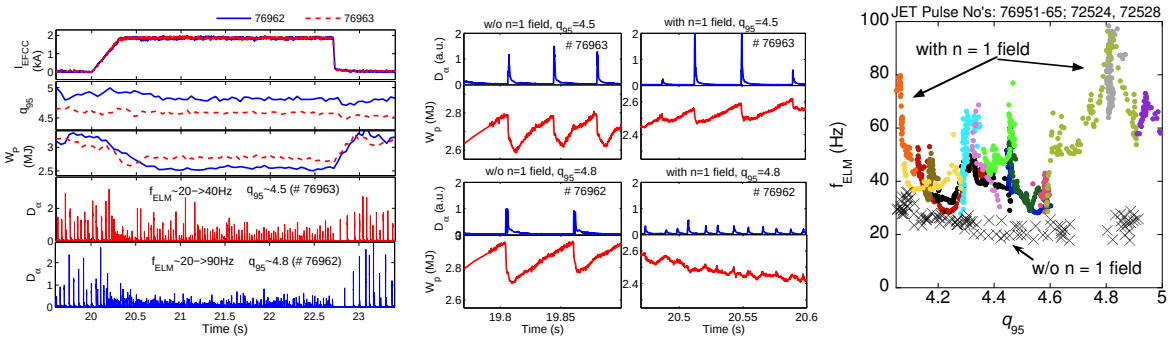

FIG. 1: Comparison of two ELM control discharges using the $n = 1$ field with different values of q_{95} of 4.5 (#76963) and 4.8 (#76962). The traces from top to bottom in the left figure are the EFCC coil current (I_{EFCC}), the edge safety factor q_{95}, the stored energy (W_p), the central line-integrated electron densities ($n_e l$), and the D_α signals measured at the inner divertor. The time traces of the intensity of D_α lines and W_p measured before and during application of $n = 1$ field are plotted for both discharges in the middle figure. ELM frequencies (f_{ELM}) as a function of q_{95} for an H-mode plasma with (closed circles) and without (crosses) $n = 1$ field are plotted in the right hand figure.

is about 10 energy confinement times. $|b_{n=1}^{r,eff}|$ calculated in the vacuum approximation is $\sim 2.5 \times 10^{-4}$ at the position of the edge pedestal. The Chirikov parameter calculated using the experimental parameters and neglecting screening of the $n = 1$ field is ~ 0.8 at $\sqrt{\Psi} = 0.925$, which indicates a weak ergodisation level at the plasma edge.

Although the same amount of effective $n = 1$ field was applied in those two discharges, f_{ELM} increased strongly by a factor of ~ 4.5 in the plasma with $q_{95} = 4.8$, while f_{ELM} increased only by a factor of ~ 2 in the plasma with $q_{95} = 4.5$. Consistent with this observation, the amplitude of $\Delta W_{ELM}/W$ also depended on q_{95} when the $n = 1$ field was applied and reduced from $\sim 7\%$ to $\sim 3.5\%$ with a non-resonant q_{95} of 4.5 and from $\sim 8.5\%$ to $\sim 2\%$ (noise level of the measurement) with a resonant q_{95} of 4.8 as shown in figure 1 (middle). Furthermore, additional drops in the plasma stored energy ($\sim 7\%$) and in the central line-integrated density ($\sim 15\%$) with the $n = 1$ fields were observed when the q_{95} was changed from 4.5 to 4.8.

Figure 1 (right) shows f_{ELM} as a function of q_{95}. Without the $n = 1$ field, f_{ELM} increases slightly from 20 to 30 Hz when q_{95} is reduced from 5 to 4. No visible large increase of f_{ELM} at any specific q_{95} was observed. However, when the $n = 1$ fields were applied, multiple peaks appeared at several narrowly separated resonant q_{95} values. The difference in q_{95} between two neighbouring resonant peaks is in the range of Δq_{95} from 0.2 to 0.3.

Figure 2 (left to right) shows the core radial profiles of plasma density, electron and ion temperature and plasma toroidal rotation measured before and after the application of the $n = 1$ fields for the two discharges shown in figure 1. Without the application of the $n = 1$ field, no visible difference was observed in the plasma core between discharges with $q_{95} = 4.8$ and with $q_{95} = 4.5$. When the $n = 1$ field was applied, a stronger reduction ($\sim 10\%$) of the plasma core density was observed in the discharge with $q_{95} = 4.8$. However, no clear difference in the effects of the $n = 1$ field on the braking of the plasma toroidal rotation or increase of ion and electron temperature was seen in-between these two discharges. Therefore, the additional drop in the total stored energy ($\sim 7\%$) in the discharge with $q_{95} = 4.8$ is mainly due to an enhancement of the density pump-out effect with a resonant q_{95} rather than a change of the electron or ion temperature. This

result indicates a strong resonant effect in q_{95} of the perturbation field on both the ELM frequency and the density pump-out.

For both discharges shown in figure 1 similar influences of the $n = 1$ fields on the core sawteeth behavior was observed. The repetition time of the sawteeth increased from ~ 0.7 s to > 1.6 s, however, no neoclassic tearing modes (NTMs) were triggered due to the sawtooth crash during ELM control with the $n = 1$ fields. A rather strong increase in the core ion temperature observed with the $n = 1$ fields could be related to the change of the sawtooth period.

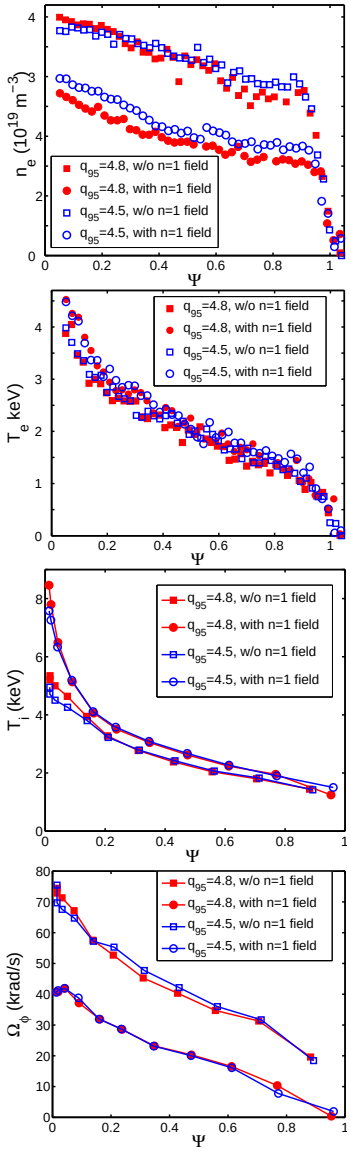

FIG. 2: Radial profiles of plasma density, electron and ion temperature, and toroidal rotation measured before and after application of the $n = 1$ field for two discharges with different q_{95}.

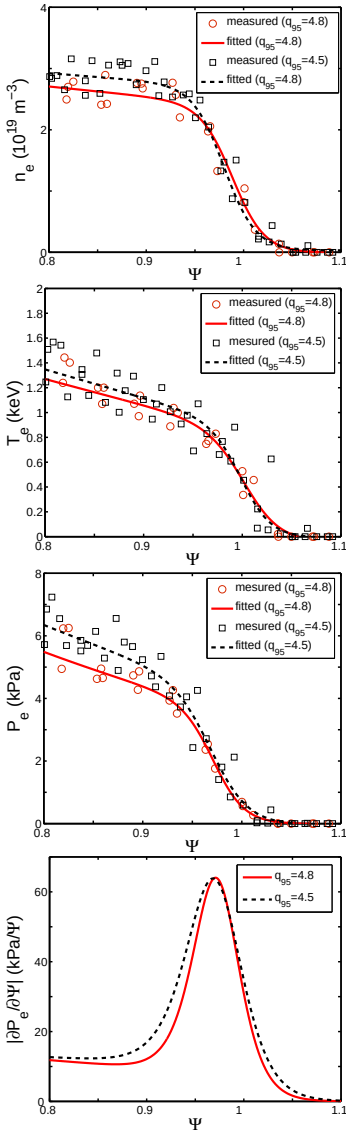

FIG. 3: Edge pedestal profiles measured before application of the $n = 1$ field for two discharges with different q_{95}.

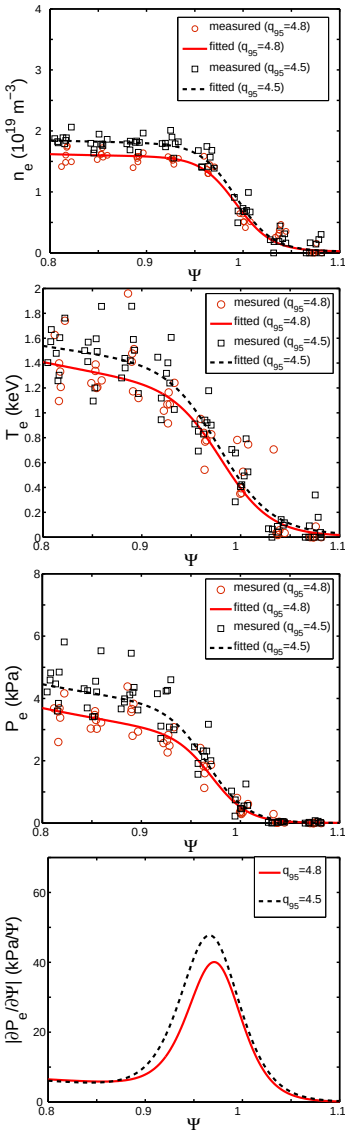

FIG. 4: Edge pedestal profiles measured during application of the $n = 1$ fields for two discharges with different q_{95}.

Without the application of the $n = 1$ fields, both the pedestal width and height

observed in the plasma with $q_{95} = 4.5$ ($I_p = 1.4$ MA) were wider and higher by $\sim 10\%$ than those observed in the discharge with $q_{95} = 4.8$ ($I_p = 1.32$ MA). This is mainly due to the differences appearing in the density pedestal rather than in the electron temperature pedestal as shown in figure 3. However, the maximal pedestal pressure gradient was not so different on changing q_{95} from 4.5 to 4.8. When the $n = 1$ field was applied, the pedestal density observed in the $q_{95} = 4.5$ discharge dropped by $\sim 28\%$, while $\sim 40\%$ drops in pedestal density were observed in the $q_{95} = 4.8$ discharge as shown in figure 4. A slight increase ($\sim 15\%$) in the pedestal electron temperature was observed in both discharges. However, because of the large reduction of the pedestal density, the increase in edge pedestal temperature was not sufficient to recover the pressure pedestal to the same height as before the $n = 1$ field application. The pressure pedestal height reduces by $\sim 20\%$ in the $q_{95} = 4.5$ case, and by $\sim 25\%$ in the $q_{95} = 4.8$ case. A significant drop in the maximal pressure gradient by $\sim 35\%$ was observed in the $q_{95} = 4.8$ case, while it was $\sim 22\%$ in the $q_{95} = 4.5$ case.

In the previous experiment, the dynamics of the edge pedestal with and without $n = 1$ field have been studied. It was found that the mitigated pedestal pressure with the $n = 1$ field recovered approximately at the same rate as without $n = 1$ field, but the ELM crash occurred earlier at a lower pedestal pressure level [14]. This result suggests that the ELM stability threshold might be reduced by the application of an $n = 1$ field. Therefore, this suggests that the ELM stability threshold in the plasma with a resonant q_{95} might be even more reduced than the one in the plasma with a non-resonant q_{95}.

2.2 Multi-resonances effect with $n = 2$ fields The multiple resonances effect in f_{ELM} vs q_{95} has also been observed with $n = 2$ fields in previous experiments on JET [13]. Recently, the power supply for the $n = 2$ EFCC configuration has been upgraded to induce a maximal I_{EFCC} up to 48 kAt (twice the previous amplitude). A further investigation of the q_{95} dependence of ELM control with an $n = 2$ field has been carried out in a wider q_{95} range from 2.8 to 5.5.

Figure 5 (left) shows an example obtained from this experiment. In this discharge, a q_{95} scan from 2.8 to 3.3 was performed during the 3 seconds flat top of EFCC current. The maximum EFCC current is 48 kAt. $|b^{r,eff}_{n=2}|$ calculated with a vacuum assumption is $\sim 1.4 \times 10^{-4}$ at the plasma edge pedestal ($\sim 44\%$ less than $|b^{r,eff}_{n=1}|$ in the experiment shown in figure 1). The time evolution of f_{ELM} indicates two peaks (~ 90 Hz and 50 Hz) in f_{ELM} appearing at $q_{95} = 2.9$ and 3.2. In between those two peaks, a minimal influence of the $n = 2$ fields on f_{ELM} (~ 30 Hz) appears at $q_{95} = 3.05$. The size of ELMs, which is indicated by a drop of pedestal T_e (ΔT_e) due to the ELM crash, follows the changes of f_{ELM}. A strong reduction of ΔT_e was observed at two resonant q_{95} values of 2.9 and 3.1. The f_{ELM} as a function of q_{95} with $n = 2$ fields applied is shown in figure 5 (right). A weaker global effect of the $n = 2$ fields on f_{ELM} is seen compared to the $n = 1$ fields, nevertheless the multi-resonance effect is clearly observed.

Compared with the previous experimental results [13], no clear changes of the resonant and non-resonant q_{95} values were observed with an increase of I_{EFCC} from 24 kAt to 48 kAt. However, with a higher amplitude of the perturbation field, f_{ELM} was increased more at all q_{95} values scanned. These experimental results also indicate that the relative increase of f_{ELM} with a low n field has a large difference at different resonant q_{95} values. The strongest increase in f_{ELM} with $n = 2$ field was observed at $q_{95} = 2.9$ and 5.4.

3 Discussion The Chirikov parameter calculated using the experimental parameters (seen in figure 1) and the vacuum approximation of the perturbation field indicates that ergodisation may only appear at the far plasma boundary ($\sqrt{\Psi} > 0.95$) as shown in figure 6. The width of the edge ergodised zone, $\delta\sqrt{\Psi}|_{\sigma>1}$ (with a Chirikov parameter, σ, larger than 1) increases slightly from 0.038 to 0.048 when q_{95} increases from 4.1 to

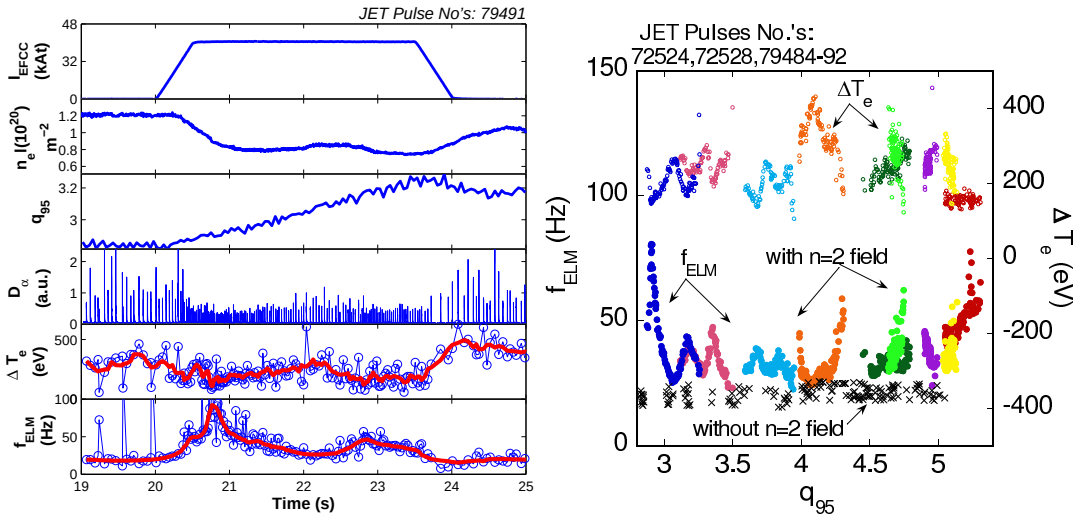

FIG. 5: (left) An example of an ELM control discharge using the $n = 2$ field with a slow ramp up of q_{95}. The time traces from top to bottom are EFCC coil current, the central line-integrated electron density, edge safety factor q_{95}, the D_α signal measured at the inner divertor, the amplitude of the periodic drops of the edge pedestal temperature due to ELMs, ΔT_e and frequency of ELMs. (right) Frequency of ELMs, f_{ELM} (closed circles) and ΔT_e (open circles) as a function of q_{95} for H-mode plasmas with $n = 2$ field. The f_{ELM} dependence on q_{95} for an identical plasma without $n = 2$ field (crosses) has been plotted as a reference.

4.8, and then saturates as q_{95} is further increased from 4.8 to 5.0. This is mainly due to a flattening distribution of the amplitudes of the Fourier components in the EFCC perturbation spectrum as show in figure 6 (left). There are no resonant features in the left graph that could explain the JET results. The mechanism of edge ergodisation, which is used to explain the ELM suppression with $n = 3$ field on DIII-D, may explain the global effect of the $n = 1$ field on f_{ELM} on JET, but it cannot explain the multi-resonance effect.

Because of rotational field screening [16], plasma rotation could affect the amplitude of the perturbation field penetrating into the plasma. However, each Fourier component (m, n) of the perturbation fields will be screened out at resonant rational surfaces ($q = m/n$). With a static perturbation field, the screening factor (s), which is defined as the ratio of the penetrated field strength to the field strength calculated using the vacuum field, strongly depends on the plasma electron perpendicular rotation ($V_{e,\perp}$) at rational surfaces. Full field penetration ($s = 1$) occurs when $V_{e,\perp}$ is zero for a non-rotating field. With a low n field, there is only a limited number of resonant rational surfaces near the edge pedestal, where both the $E \times B$ plasma rotation and the diamagnetic drift are relatively large. In addition, the number of edge resonant rational surfaces for the $n = 2$ field should be twice as high as for the $n = 1$ field. However, comparison of the multi-resonance effect observed with $n = 1$ and $n = 2$ fields in a q_{95} window of 4 to 5 shows that the values of q_{95} at the resonances are similar. Therefore, the plasma rotational field screening effect by itself can not explain this effect.

A possible explanation of the multi-resonance effect has been proposed using the ideal external peeling mode/relaxation model [15]. In this model it is assumed that an unstable ideal external peeling mode triggers a turbulent relaxation process which produces a post-ELM relaxed force-free configuration [17] that is stable to all possible external peeling modes. The flattening of the current profile by the relaxation process generally produces an increase in the edge current density which in itself further destabilises the peeling

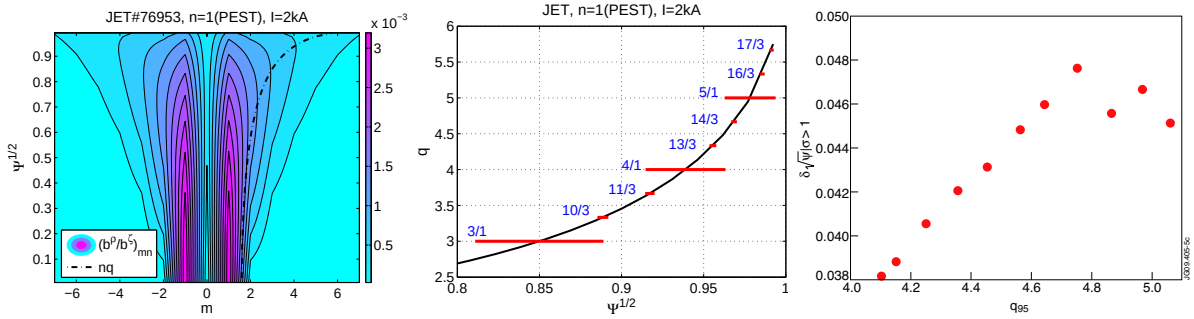

FIG. 6: (left) Radial component of the $n = 1$ helical mode spectrum for $n = 1$ EFCC configuration with $I_{EFCC} = 2$ kA using vacuum fields. Here the x-axis is the poloidal mode number, m. The calculation is based on an equilibrium reconstruction for JET pulse #76953 with q_{95} of 4.8 (similar to the discharge #76962 shown in figure 1). Pitch resonant modes with $m = nq(\Psi)$ are shown by the (black) dashed line. (middle) Radial profile of safety factor q for pulse #76953. The locations and widths of islands calculated with a vacuum assumption are superposed on the plot. (right) Width of the edge ergodisation zone, $\delta\sqrt{\Psi}|_{\sigma>1}$,with a Chirikov parameter, σ, larger than 1 as a function of the edge safety factor q_{95} using the vacuum approximation.

mode; however this is countered by the formation of a stabilising negative edge current sheet, and it is the balance of these two effects that determines the predicted width of the relaxed region. Unlike the ballooning mode, the peeling mode does not depend on toroidicity to be unstable and is driven by edge current density. In a simple cylindrical model, the plasma is peeling unstable whenever [18]

$$\Delta^{'}(1/q_a - n/m) + J_a > 0 \ , \tag{1}$$

where m is the poloidal mode number, $\Delta^{'}$ is the jump in $(r/b_r)db_r/dr$ across the plasma-vacuum interface (b_r is the perturbed radial field) which encapsulates information about the equilibrium current profile ($\Delta^{'} = -2m$ for a vacuum response [18]), and J_a is the driving edge current density (normalised to the on-axis value). A similar criterion can be obtained for an arbitrarily shaped toroidal plasma [19].

In the peeling/relaxation model [15, 18], the ELM width (the extent of the relaxed region, d_E) is determined by requiring that external peeling modes are stabilised for all modes (m, n). Hence, for a given current profile, the mode (m, n) requiring the largest d_E determines the width. A key quantity in the calculation of d_E is the $\Delta = (1/q_a - n/m)$ of Eq. 1, and as m and n must be integers, Δ exhibits detailed structure. It is indeed this fact that gives rise to the 'resonances' in the model predictions.

The dominant unstable peeling mode also depends on the normalised edge current, J_a. Multiple resonances naturally exist at small edge current density [18], while for larger J_a the low n modes given by Eq. (1) dominate over extended regions of q_a and multiple resonances disappear. Taking the ELM repetition time to be the time for the relaxed state to diffuse in a classical manner back to the initial state, a simple qualitative measure of the ELM frequency is given by $f \sim 1/d_E^2$, and this is plotted for both low edge current density and high edge current density cases in figure 7.

4. Conclusion. The multi-resonance effect in f_{ELM} vs q_{95} has been observed with either an $n = 1$ or an $n = 2$ magnetic perturbation field on JET. At the resonant q_{95} a strong increase in f_{ELM} and an enhancement of the density pump-out effect has been observed. A strong reduction in the maximal edge pressure gradient by $\sim 35\%$ has been found in the discharge with a resonant q_{95} while there is $\sim 22\%$ reduction in the non-resonant q_{95} case. The multi-resonance effect has been studied with the $n = 2$ fields in a

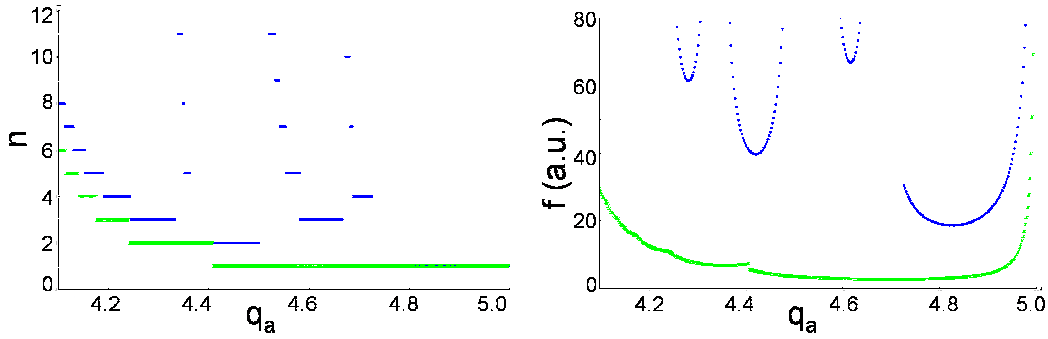

FIG. 7: Model predictions of ELM frequency and trigger n number against edge q_a for two cases with different normalized edge current density, $J(a)/J(0)$, of (blue) 0.075 and (green) 0.35.

wider range of q_{95}. An increase in ELM frequency by a factor of ~ 4.5 has been observed with a resonant q_{95} of 2.9. The relative increase of ELM frequency with a low n field can have a large difference at different resonant q_{95} values. A model in which the ELM width is determined by a localised relaxation to a profile which is stable to peeling modes can qualitatively predict this multi-resonance effect with a low n field. The dominant unstable peeling mode number and f_{ELM} depends on the amplitude of the normalized edge currents as well as q_{95}.

This work, supported by the European Communities under the contract of Association between EURATOM and FZJ, was carried out within the framework of the European Fusion Development Agreement. The views and opinions expressed herein do not necessarily reflect those of the European Commission.

[1] F. Wagner, *et al.*, Phys. Rev. Lett. **49**, 1408 (1982).
[2] A. Loarte, *et al.*, J. Nucl. Materials **313-316**, 962 (2003).
[3] G. Saibene, *et al.*, Nucl. Fusion **45**, 297 (2005).
[4] P. T. Lang, *et al.*, Nucl. Fusion **44**, 665 (2004).
[5] J. W. Connor, Plasma Phys. Control. Fusion **40**, 531 (1998).
[6] H.R. Wilson, *et al.*, Phys. Rev. Lett. **92**, 175006 (2004).
[7] T. E. Evans, *et al.*, nature physics **2**, 419 (2006).
[8] T. E. Evans, *et al.*, Nucl. Fusion **45**, 595 (2005).
[9] Y. Liang, *et al.*, Phys. Rev. Lett. **98** 265004 (2007).
[10] Y. Liang, *et al.*, Plasma Phys. Control. Fusion **49** B581 (2007).
[11] B. V. Chirikov, Phys. Rep. **52**, 263 (1979).
[12] Y. Liang, *et al.*, Nucl. Fusion **50** 025013 (2010).
[13] Y. Liang, *et al.*, Phys. Rev. Lett. **105** 065001 (2010).
[14] Y Liang, *et al.*, Proceeding of 19th ITC conference, (to be published in Plasma and Fusion Research), (2010).
[15] C. G. Gimblett, R. J. Hastie and P. Helander, Phys. Rev. Lett., **96**, 035006-1-4 (2006).
[16] M. Becoulet, *et al.*, Nucl. Fusion **48**, 024003 (2008).
[17] J. B. Taylor, Rev. Mod. Phys., **58**, 741 (1986).
[18] C. G. Gimblett, R. J. Hastie and P. Helander, Plasma Phys. Control. Fusion, **48**, 1531 (2006).
[19] A. J. Webster and C. G. Gimblett, Phys. Rev. Lett., **102**, 035003 (2009).